Depth Sizing of Surface Breaking Flaw on Its Open Side by Short Path of Diffraction Technique

Hiroyuki FUKUTOMI, Shan LIN and Takashi OGATA
Central Research Institute of Electric Power Industry
2-11-1 Iwatokita, Komae, Tokyo 201-8511, JAPAN
Tel: +81-3-3480-2111, Fax: +81-3-3430-2410
E-mail: fukutomi@criepi.denken.or.jp, Web: http://criepi.denken.or.jp/en/

Abstract

Central Research Institute of Power Industry has developed a highly accurate and low cost flaw depth sizing technique which is easy-to-use in comparison to standard techniques such as crack tip diffraction and TOFD techniques. This technique is called the short path of diffraction (SPOD) technique. In this technique, an angle beam transducer and a 0-degree transducer are used to excite and receive waves. So far the applicability of SPOD to depth sizing on flaw open side has not been discussed. This paper deals with the effectiveness of SPOD in this application. Finite element modeling for wave propagation revealed that two echoes were obtained which were obviously related to the tip and opening of a surface breaking flaw in SPOD configuration. Based on this result, an equation was derived to calculate the flaw depth from the difference of the relative beam paths. To demonstrate the applicability of SPOD to surface breaking flaws, depths of fatigue cracks introduced in stainless steel blocks were measured. Because the depths measured were in excellent agreement with actual ones, SPOD could be applied to flaw depth sizing on its open side.

Keywords: Ultrasonic Testing, Surface Breaking Flaw, Flaw Depth Sizing, Short Path of Diffraction Techniques

1. Introduction

For assessing fitness for duty, accuracy of sizing stress corrosion cracks (SCC) has been required to be improved in the welds of pipes in nuclear power stations [1]. Also, long-term operated fossil power stations have faced problems with creep damage of high energy pipes. The pipe burst occurring from this damage has been reported [2, 3]. In order to assure the integrity of structural components and avoid such a catastrophic failure, high accuracy nondestructive inspection is required for detection and sizing of flaws in welds of thick-walled pipes. Nondestructive inspection by ultrasonic testing is being used to develop more accurate sizing techniques. The special attention is being paid to phased array transducers and the Time of Flight Diffraction (TOFD) technique [4, 5].

Difficulties are often encountered when performing ultrasonic testing of thick-walled austenitic stainless steel welds. The primary causes of these problems are known to be regular, crystalline atomic structure. An ultrasonic wave traveling through such an inhomogeneous and anisotropic material suffers

beam path bending, attenuation due to scattering at grain boundaries, and beam profile distortion [6-9]. TOFD cannot be easily applied to such specimens with high accuracy of flaw depth measurement. The difficulty to identify the tip echo buried in unexpected echoes from the weld needs the experienced inspector [10].

Central Research Institute of Power Industry has developed a new pit-catch technique for accurate flaw depth to tackle the disadvantage of techniques mentioned above. The new pit-catch technique arranges an angle beam transducer and a 0-degree transducer to detect diffracted waves that travel in the shortest path for flaw depth sizing, and is called as the Short Path of Diffraction (SPOD) technique [11]. Effectiveness of SPOD has been demonstrated by applying to depth sizing of surface breaking flaws on back side. This paper deals with applicability of SPOD to front surface flaws.

2. Flaw depth sizing by SPOD

Flaw depth sizing can be easily made with a longitudinal or shear angle beam transducer and the longitudinal 0-degree transducer as shown in figure 1. When the 0-degree transducer is placed directly over a flaw, the diffracted wave with the shortest beam path can be observed. Therefore, the attenuation by scattering and beam spreading would be lowered and strong echoes from longitudinal waves diffracted directly at the flaw tip and waves traveling near the flaw surface would be detected. A directly diffracted longitudinal wave, L_1 , and a surface longitudinal wave traveling near the flaw surface before reflecting at the back wall, L_2 , with beam paths of W_1 and W_2, respectively, can be detected by a longitudinal 0-degree transducer placed over the flaw. With this transducer arrangement the flaw depth, d, is simply half of difference between W_1 and W_2, that is

$$d = \frac{1}{2}(W_2 - W_1) . \tag{1}$$

Consider depth sizing of surface breaking flaws on their open sides as shown in figure 2. With this test configuration, flaw depth, d_s, can be calculated by

$$d_s = \frac{1}{2W}\left(W^2 - S^2\right), \tag{2}$$

where W is the beam path of tip diffraction echo, and S is the transducer separation. Without calibration of beam path in an ultrasonic testing instrument, the wedge delay of angle beam transducer has to be measured because the readings include the wedge delay. Assuming that the echo due to a refracted at an flaw opening is observed, the difference between echoes due to the waves diffracted at a flaw tip and refracted at an flaw opening, ΔW, is given as

$$\Delta W = W - S \tag{3}$$

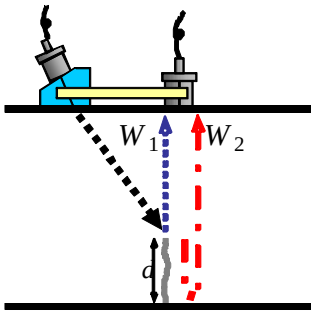

Figure 1 Depth sizing of back surface flaw

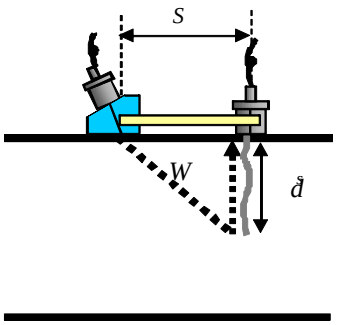

Figure 2 Depth sizing of front surface flaw

because the relative beam path is identical to S when the 0-degree transducer locates over the flaw. Using equations (2) and (3), d_s can be obtained as

$$d_s = \frac{\Delta W^2 + 2\Delta W}{2(\Delta W + S)}, \tag{4}$$

without measuring the wedge delay.

3. Finite element modeling

In order to investigate the effectiveness of SPOD to depth sizing of surface breaking flaws on their open sides, finite element computations were carried out. A computation model was shown in figure 3, where two assumptions were made. They were plane strain and free boundary condition for all boundaries in this figure. On the upper surface, there were transmitting and receiving domains. Vertical forces were loaded at the transmitting domain to generate ultrasonic waves. The loading time varied with lateral position on the surface to generate a longitudinal refracted angle of 70 degrees, in this computation. The central frequency of the incident wave was 5 MHz. A-scan waveforms were calculated from displacements at the receiving domain. Also, there were a slit opening to the upper surface. The material constants in computation were used, assuming the test specimen was stainless steel. Considering computation efficiency and solution convergence, integration time step t and mesh size h are restricted as

$$h \le 1/16\lambda, \quad t \le 0.3t_h \ , \tag{5}$$

where □ is the wavelength of a shear wave and t_h is

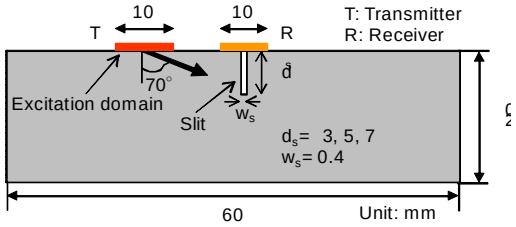

Figure 3 Computational model

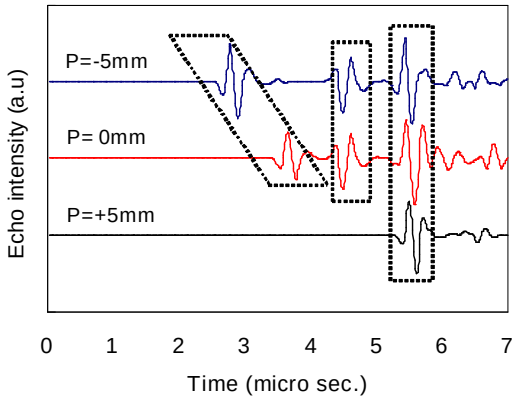

Figure 5 Echoes due to slit with different 0-degree transducer positions

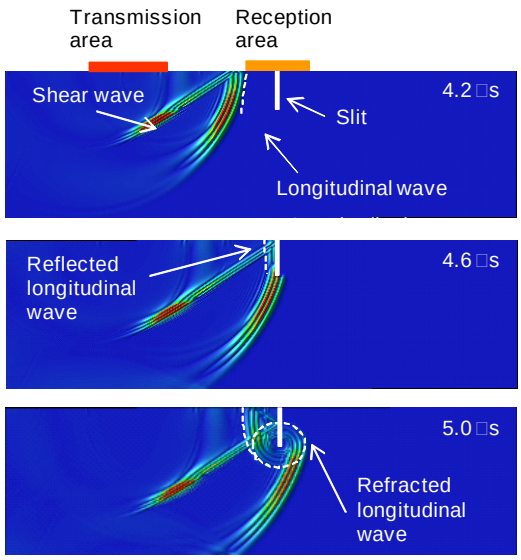

Figure 4 Wave front around slit from angle beam transducer

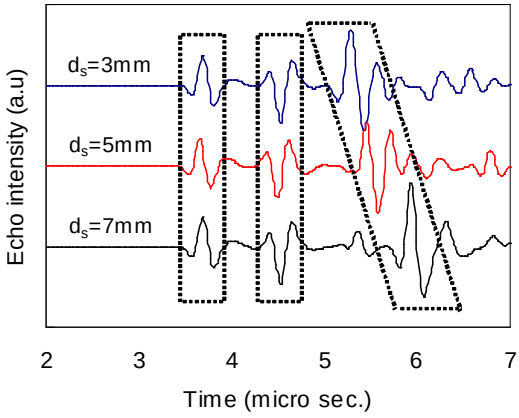

Figure 6 Echoes due to slits with different depths

the propagation time of a shear wave through distance *h*.

Figure 4 shows wave propagation at 3.6, 4.6 and 5.0 μs. As shown in this figure, shear and longitudinal waves were excited, and propagated toward the lower surface. After the longitudinal wave was diffracted at the tip of slit, its diffracted wave was received by the receiving domain. Predicted waveforms with a slit 5 mm deep are shown in figure 5 as only the 0-degree transducer was moved to right and left. P = 0 mm, 5mm and -5 mm stand for positions where the transducer was located over the slit and moved to right and left. There echoes, L_s, L_o and L_t, in this figure, arose from the lateral wave and waves reflected at the slit opening and diffracted at the slit tip, respectively. Slit depths are 5.0 mm and 4.8 mm, calculated from equation (4) and the waveforms at P = 0 mm and -5 mm. Figure 6 shows waveforms corresponding to slits with depths of 3 mm, 5 mm, 7 mm at P = 0 mm. The beam path difference between L_o and L_t varied according to the slit depth. The depth calculated from equation (4) was compared with the actual depth in figure 7. Because the calculated depth is in excellent agreement with the actual depth, equation (4) is expected to be useful.

4. Experimental results

In order to verify the sizing accuracy of SPOD, a test was performed using a 0-degree transducer as a receiver and the longitudinal angle beam transducer at a refraction angle of 70 degrees as a

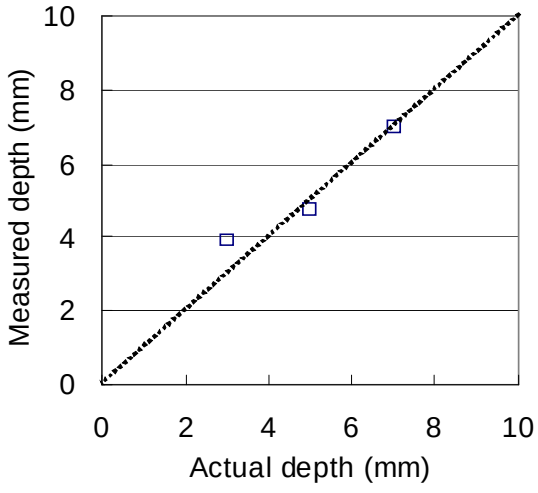

Figure 7 Comparison between actual depth and depth calculated from predicted

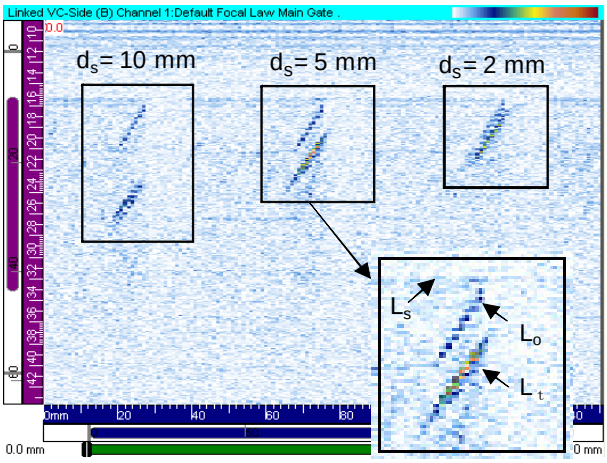

Figure 8 B scan image of slits in SPOD

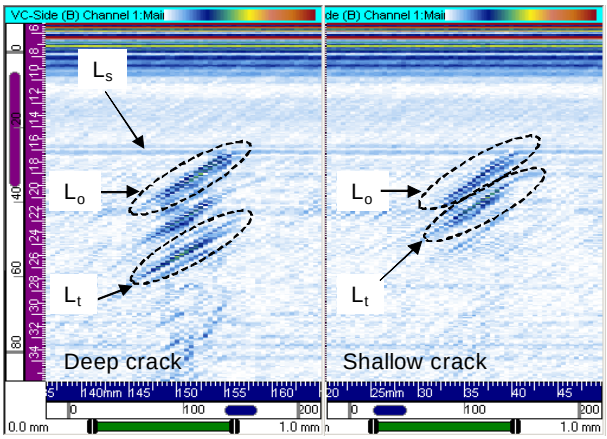

Figure 9 B scan image of fatigue cracks in SPOD

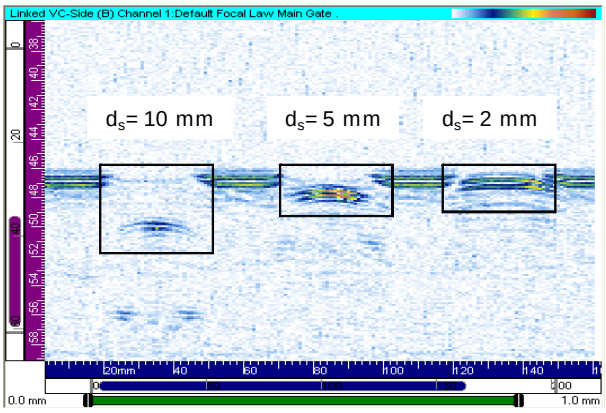

Figure 10 B scan image of slits in TOFD

transmitter. The central frequency and piezoelectric element diameter of transducers were 5 MHz and 10 mm. Setting the transducer separation to 18 mm, line scans were taken on the fat and smooth surface of stainless steel block where slits with depths of 2, 5 and 10 mm and a width of 0.3 mm were machined and fatigue cracks were induced. The ultrasonic measurement system consisted of a commercial ultrasonic instrument and a scanner. Glycerin paste was used as the couplant.

B-scan images of the slit and fatigue crack are shown in figures 8 and 9. Clear indications due to L_o and L_t were identified, and ΔW of each slit or fatigue crack was almost kept constant against transducer position variation when the relative indications appeared. For comparison, TOFD measurement was made under conditions about the as the SPOD measurement. As shown in figure 10, it might be difficult to detect slit 2 mm if inspection surface is rough and the refractor is a natural flaw instead of a slit. In figure 11, depths measured by SPOD were compared with actual depths. The depth of fatigue crack was observed by a microscope on the surface of a polished cut, by sectioning the stainless steel on scanning potions. SPOD shows excellent performance for sizing depths in stainless steel. SPOD can be also applied to other typical structural materials, such as carbon steel or chromium alloy steel.

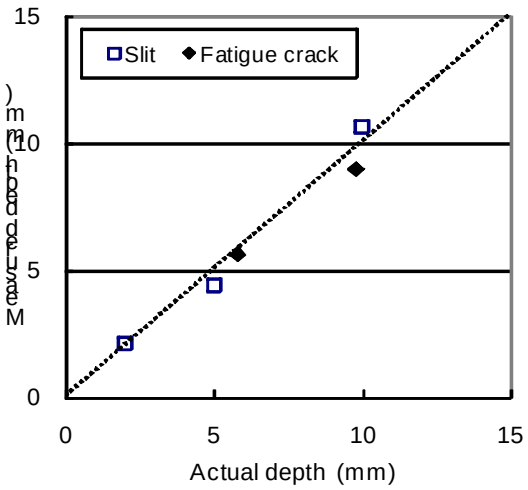

Figure 11 Comparison between actual and measured depths of slit and fatigue crack

5. Conclusions

Application of SPOD to depth sizing of surface breaking flaws on their open sides was discussed in this study. After deriving a simple equation for calculating depth from beam path lengths from geometrical relationship between transducers and a flaw, finite element computations of wave propagation for SPOD were performed to investigate the possibility of depth sizing. Numerical results showed that echoes arising from waves reflected at the slit opening and diffracted at the slit tip were observed, whose beam path difference was related to the slit depth. In order to demonstrate effectiveness of SPOD, experimental measurements were conducted with machined slits and fatigue cracks. Their depths measured were in excellent agreement with the actual depths. Therefore SPOD is expected to be useful for the nondestructive inspection of power generation components.

References

[1] C. D. Cowfer and O. F. Hedden, Journal of Pressure Vessel Technology, Transactions of the ASME, Vol. 113, 1991, pp. 170-173.

[2] F.V. Ellis and R. Viswanathan, Proc. ASME PVP Conference, PVP-Vol.380, Fitness-for Service Evaluations in Petroleum and Fossil Power Plants, ASME, 1998, pp.59-76.

[3] J.F. Henry, G. Zhou and C.T. Ward, Proceedings of Conference on Advances in Life Assessment and

Optimization of Fossil Power Plants, March 2002, (EPRI/DOE).

[4] H. Fukutomi, S. Lin and T. Ogata, CRIEPI Report, Q04016, 2005.

[5] S. Lin, H. Fukutomi and T. Ogata, CRIEPI Report, Q04015, 2005.

[6] A.H.Haker, J.A.Ogilvy and J.A.G.Temple, Journal of Nondestructive Evaluation, Vol.9, No.213, 1990, p.155-165.

[7] S.Ahmed and R.B.Thompson, Nondestrutive Testing and Evalution, Vol.8-9, 1992, pp.523-531.

[8] J.A.Ogilvy, Ultrasonics, Vol.24, No.11, 1986, pp.337-347.

[9] J.A.Ogilvy, NDT International, Vol.18, No.2, 1985, pp.67-77.

[10] J.R.Tomlinson, A.R.Wagg and M.J.Whittle, British Journal of NDT, 1980, pp.119-127.

[11] S. Lin, H. Fukutomi and T. Ogata, Review of Progress in Quantitative Nondestructive Evaluation, 26, 2006, pp.103-109.